Preparation and Properties of UV-curable Organic/Inorganic Hybrid Nanocomposites Based on Layered Double Hydroxides

Yan Yuan, Wenfang Shi/CAS Key Laboratory of Soft Matter Chemistry, Department of Polymer Science and Engineering, University of Science and Technology of China, Jinzhai Road 96, Hefei, Anhui 230026, P. R. China

Abstract

The exfoliated polymer/layered double hydroxide (LDH) nanocomposites based on MgAl were prepared through intercalating a photoinitiator, 2-hydroxy-2-methyl-1-phenylpropane-1-one (1173), or grafting an acrylated coupling agent, 3-(methyl-acryloxy)propyltrimethoxysilane (KH570), forming LDH-1173 or LDH-KH, following by blending with a commercial acrylate oligomer and a monomer, and then exposed to a UV lamp. It was found from the XRD, TGA and Photo-DSC analysis that the LDH-1173 effectively initiated the photopolymerization of formulation, forming the exfoliated polymer/LDH nanocomposite. However, the intercalated polymer/LDH nanocomposite was obtained for the system with additional 1173 except for LDH-1173 addition. On the other hand, the LDH-KH blend was UV-cured in the presence of 1-hydroxycyclohexyl-phenyl ketone as a photoinitiator, reaching to the high photopolymerization rate and unsaturation conversion. The XRD patterns indicated the formation of exfoliated microstructures. The TEM and HR-TEM observation for both systems exhibited the fine dispersion and random orientation of LDHs in the polymer matrices. Compared with the pure polymer material, both the exfoliated and intercalated polymer/LDH nanocomposites exhibited the enhancements in the mechanical and thermal properties, as well as hardness.

Keywords: Layered double hydroxide (LDH); UV curing; Nanocomposite; Property

1. Introduction

In recent years, polymer/layered crystal nanocomposites have drawn more and more attention because of their unique properties, such as improved mechanical, thermal, and gas barrier properties, reduced flammability, and enhanced chemical stability [1-5]. However, many studies focus on polymer/layered silicate systems, while the artificial layered double hydroxide (LDH) systems have been less reported in literature [6-8].

The LDH can be represented by the ideal formula, $[M^{2+}_{1-x}M^{3+}_{x}(OH)_2]^{x+}A^{n-}_{x/n}\cdot mH_2O$, where M^{2+} and M^{3+} are divalent and trivalent metal cations, such as Mg^{2+}, Al^{3+}, respectively, and A^{n-} is an exchangeable anion, such as CO_3^{2-}, SO_4^{2-}, and NO_3^{-}. The much higher charge density and stronger interaction in LDHs than layered silicates make the exfoliation of LDHs much more difficult [9-11]. To improve the affinity of LDHs towards organic materials, much efforts focus on the modification of LDHs with some organic or polymeric anions, such as alkyl sulfates, alkyl sulfonates, phenyl phosphates and so on [1,12-15]. Hsueh et al. [16] reported the preparation of epoxy/LDH

nanocomposite by thermally polymerization based upon the intercalated LDH with amino laurate. Because of the reaction between amine group and epoxy group, the exfoliated epoxy/LDH nanocomposite was easily obtained.

In this study, the preparation of exfoliated UV cured polymer/LDH nanocomposites is reported. For obtaining completely exfoliated nanocomposites, the adoptable method is to prepare the intercalated LDHs with reactive groups, which enhances the polymerization in interlayer. Therefore, 2-hydroxy-2-methyl-1-phenylpropane-1-one (1173) reacts firstly with isophorone diisocyanate (IPDI) to obtain the semiadduct IPDI-1173, which is further introduced into the interlayer of LDH. On the other hand, a acrylated silane coupling agents, 3-(methyl-acryloxy)propyl trimethoxysilane (KH570), is chosen to supply the methacrylate group. To prepare an exfoliated polymer/LDH nanocomposite, sodium dodecyl sulfate (SDS) and KH570 both are intercalated into the LDH through the coprecipitation method for introducing the methacrylate group into the interlayer of LDH.

The obtained intercalated LDH-1173 or LDH-KH is formulated with a commercial acrylate monomer and an oligomer, and then exposed to a UV lamp, forming the exfoliated polymer/LDH nanocomposite. The mechanical and thermal properties, and microstructures of UV cured nanocomposites are investigated.

2. Experimental

2.1. Materials

Sodium dodecyl sulfate (SDS), dimethylacetamide (DMAC), isophorone diisocyanate (IPDI), di-n-butyltin dilaurate (DBTDL), $Mg(NO_3)_2{\cdot}6H_2O$, $Al(NO_3)_3{\cdot}9H_2O$ were all purchased from Sinopharm Chemical Reagent Co. (Shanghai, China). 3-(Methyl-acryloxy)propyltrimethoxysilane (KH570) was purchased from Nanjing Yudeheng Fine Chemical Co. (China). Aminoundecanoic acid (AD) was purchased from Sigma-Aldrich Co. (USA). EB270 was supplied by Cytec Industries Inc. (USA). 1,6-Hexamethyldiol diacrylate (HDDA) was supplied by Eternal Chemicals Co. (Taiwan). 2-Hydroxy-2-methyl-1-phenylpropane-1-one (1173) and 1-hydroxycyclohexyl-phenyl ketone (Rutecure 1104) was provided by Runtec Chemicals Co. (Changzhou, China). All the materials were used without further purification except for IPDI and KH570, which were distilled before used.

2.2. Preparation

The coprecipitation method was used for obtaining the modified LDH with AD (LDH-AD) as a milk-white suspension according to the literature [1].

For obtaining the intercalated LDH with 1173 (LDH-1173), the following process was carried out. A proper amount of LDH-AD water suspension was dispersed in toluene. Then water was removed by azeotropy, obtaining a LDH-AD toluene suspension. The mixture of 1173 and DBTDL in toluene was dropped slowly into IPDI under stirring at 0 °C, and reacted at 50 °C for obtaining 1173-IPDI. Then LDH-AD dispersion in toluene was added into 1173-IPDI, and stirred. The product, named LDH-1173, was collected by filtering and repeatedly washed with toluene to remove the unreacted 1173-IPDI.

For obtaining the modified LDH with KH570 (LDH-KH), the following process was performed. Firstly, the LDH-DS toluene suspension was prepared by the coprecipitation method of LDH with SDS reported in the literature [16], and mixed with DMAC under vigorously stirring at 100 °C. Then toluene was removed under vacuum. KH570, a proper amount of catalyst (0.1 wt% DBTDL) and p-hydroxyanisole were added into DMAC suspension of LDH-DS and stirred at 120 °C for different times (12, 24 and 36 h), respectively, under N_2 atmosphere. The crude product was filtrated and

washed with toluene to remove the unreacted KH570. The toluene suspensions of LDH modified by both DS and KH570 were obtained and named LDH-KH-12, LDH-KH-24 and LDH-KH-36 for different reaction times.

The primary formulations utilized in this study were consisted of EB270:HDDA (7/3) and LDH-1173 in the respective concentration of 1, 3 and 5 wt%. A desired amount of LDH-1173 toluene suspension was first dispersed in EB270/HDDA mixture. After stirring to achieve a complete dispersion, toluene was removed under vacuum. Then every formulation was divided into two samples, including one without additional 1173, referred as a-1, a-3 and a-5 (series A), and the other added with additional 3 wt% 1173, and referred as b-1, b-3 and b-5 (series B). And the pure polymer film as reference was obtained by EB270/HDDA (7:3) with 3wt% 1173 addition.

With the LDH-KH system, the LDH-KH-24 was added into the primary formulation with the respective concentration of 1, 3 and 5 wt%, obtaining the UV-curable urethane diacrylate/LDH blends, named LK1, LK3 and LK5, respectively. After stirring to achieve a complete dispersion, toluene was removed under vacuum. Then 2% radical fragmental photoinitiator (Runtecure 1104) was added and stirred. The pure polymer as reference was obtained by EB270/HDDA (7:3) with 2 wt% Runtecure 1104.

2.3. UV curing

The formulations were exposed to a medium pressure mercury lamp (1 kW, Fusion UV systems, USA) with the band conveyer speed of 1.6 m min^{-1} to obtain the UV cured polymer/LDH nanocomposites.

2.4. Measurements

The XRD patterns were recorded using a Rigaku D/Max-rA rotating anode X-ray diffractometer. The TEM and HR-TEM micrographs were obtained with a Hitachi (Tokyo, Japan) H-800 and JEOL-2011, respectively. The samples were ultramicrotomed with a diamond knife on a LKB Pyramitome to give 60 nm thick slices. The TGA was performed on a Shimadzu TGA-50H thermoanalyzer. The photopolymerization rate was monitored in air by a CDR-1 DSC equipped with a UV spot cure system BHG-250. The incident light intensity at the sample pan was measured to be 2.4 mW cm^{-2} with a UV power meter. The tensile storage modulus and tensile loss factors of UV cured films were measured by a dynamic mechanical thermal analyzer (Diamond DMA, PE Co., USA) at a frequency of 10 Hz and a heating rate of 5 °C min^{-1} in the range of -100 to 200 °C with the sheets of 25×5×1 mm^3. The crosslink density as the molar number of elastically effective network chain per cube centimeter of the film was calculated from the storage modulus in the rubbery plateau region. The mechanical properties were measured with an Instron Universal tester (model 1185, Japan) at 25 °C with a crosshead speed of 25 mm min^{-1}. The pendulum and pencil hardness were determined in Persoz mode in seconds by using a QBY pendulum apparatus, and a QHQ-A pencil hardness apparatus (Tianjin Instrument Co., China), respectively.

3. Results and discussion

3.1. Characterization

The XRD patterns for MgAl-LDH, LDH-AD, LDH-1173 and UV cured polymer/LDH nanocomposites are shown in Fig. 1. The unmodified MgAl-LDH shows a basal spacing of 0.78 nm ($2\theta = 11.6°$), while the LDH-AD shows a basal spacing of 2.30 nm ($2\theta = 3.8°$). The enlarged spacing of LDH-AD indicates that AD was successfully intercalated into MgAl-LDH. After 1173-IPDI

reacted with LDH-AD, the basal spacing increases from 2.30 nm to 4.88 nm. This indicates that LDH-1173 as a new complex photoinitiator had been successfully synthesized. Moreover, for the UV cured polymer/LDH nanocomposites a-5 containing 5% LDH-1173 and b-5 with additional 1173, no XRD diffraction was observed, compared to the basal spacing of 4.88 nm (2θ= 1.8°) for LDH-1173. Though the absence of XRD diffraction peak doesn't mean the occurrence of completely exfoliation, it can indicate that the random orientation has happened for a-5 and b-5.

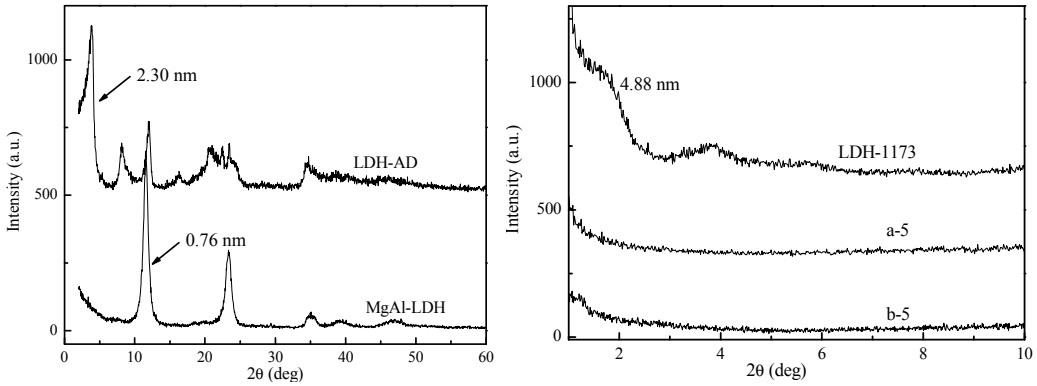

Fig. 1. XRD patterns of MgAl-LDH, LDH-AD, LDH-1173 and UV cured polymer/LDH nanocomposites.

Fig. 2 shows the XRD patterns for LDH-DS and LDH-KH. The LDH-DS shows a basal spacing of 2.67 nm (2θ = 3.3°), while the LDH-KH-12, 24 and 36, respectively, show the basal spacing of 2.53 nm (2θ = 3.5°), 2.41 nm (2θ = 3.7°) and 2.34 nm (2θ = 3.8°). As the grafting time prolonged, the space of the interlayer became smaller, contrarily. This can be explained that a part of DS was exchanged out of the interlayer when KH570 was grafted into the LDH-DS, considering the monolayer length of DS (~2.08 nm) is greatly larger than that of KH570 (~1.10 nm). Therefore, as the content of grafting KH570 increases, the basal spacing of LDH-KH decreases.

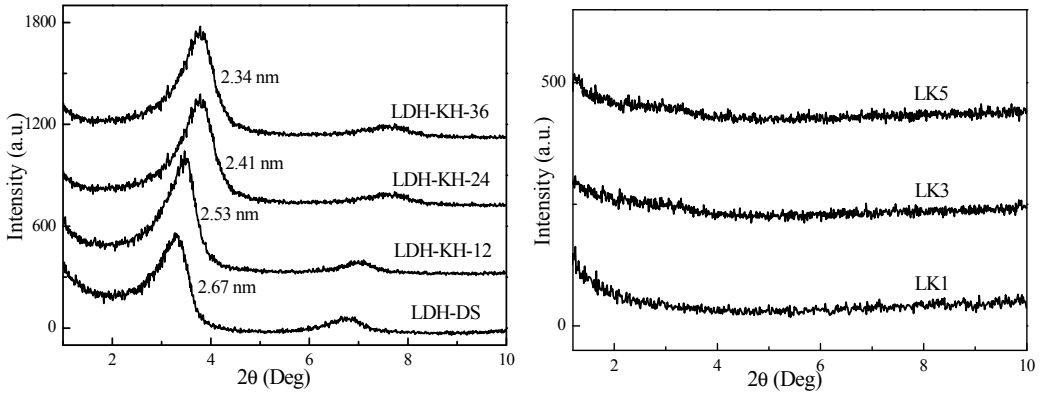

Fig. 2. XRD patterns of LDH-DS, LDH-KH, and UV cured polymer/LDH nanocomposites.

The TGA in N_2 atmosphere was used to determine the contents of organo-modifier and other volatile materials (e.g. water) in the sample. From the TGA curves, as shown in Fig. 3, for MgAl-LDH, the weight loss of 13.8% below 200 °C was attributed to the loss of physically adsorbed and interlayer water. However, at above 200 °C, the weight loss of 28.5% was ascribed to the dehydroxylation of LDH layers with the elimination of NO_3^- and CO_3^{2-}. For LDH-AD and LDH-1173, the weight loss of 13.8% and 5%, respectively, below 200 °C was also related to the loss

of physically adsorbed and interlayer water. At above 200 °C, the weight loss of 49% for LDH-AD and 77.4% for LDH-1173 was resulted from the decomposition and combustion of the intercalated organo-modifiers. Heating to 600 °C, the smallest amount of residual of 17.6% for LDH-1173 was obtained compared with MgAl-LDH and LDH-AD, indicating that the LDH-1173 was successfully synthesized.

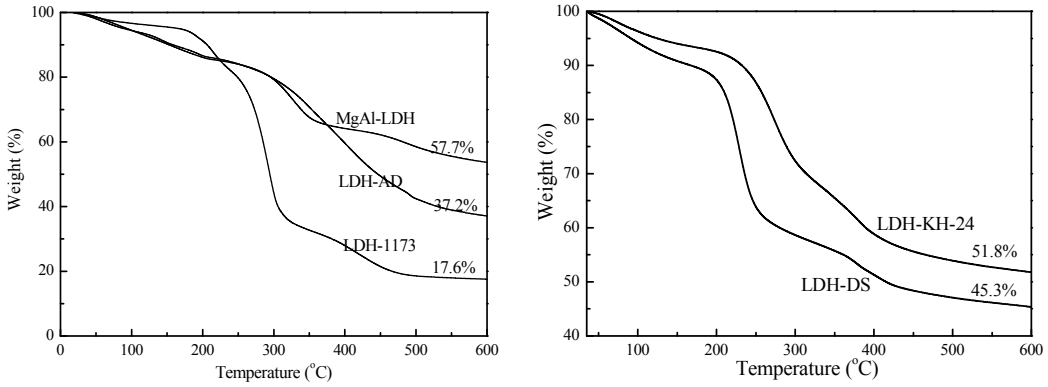

Fig. 3. TGA curves of MgAl-LDH, LDH-AD, LDH-1173, LDH-DS and LDH-KH-24.

As the TGA curves shown in Fig. 3, for the LDH-DS and LDH-KH-24 TGA, the weight loss below 200 °C is related to the loss of physically adsorbed and interlayer water. At above 200 °C, the weight loss of 42% for LDH-DS and 40.7% for LDH-KH-24 should be due to the decomposition and combustion of the intercalated organomodifiers. After heating to 600 °C, the weight residuals for LDH-DS and LDH-KH-24 are 45.3% and 51.8%, respectively, indicating that the modified LDH-DS and LDH-KH were obtained.

3.2. Photopolymerization behavior initiated by LDH-1173

Fig. 4 shows the photopolymerization rates at the peak maximum (R_p^{max}) and the final double bond conversion (P^f) of formulation series A (a-1, a-3, a-5) and series B (b-1, b-3, b-5), respectively. From the figures, it can be seen that the formulation using 1173 as a photoinitiator has the highest R_p^{max} and the shortest irradiation time to reach the R_p^{max}. The lower concentration of double bond and the higher viscosity, compared with the formulation without LDH addition, result in the lower R_p^{max} and the longer irradiation time to reach R_p^{max}, as well the P^f. However, for the series A with only LDH-1173 addition as a photoinitiator, the R_p^{max} and P^f increase distinctly with increasing the content of LDH-1173. This is due to the increase of photoinitiator 1173 in the formulation as the LDH-1173 loading increased. This result indicates that the 1173 intercalated into the LDH interlayer has the ability to initiate the photopolymerization of acrylate resin, although not effective as using pure 1173.

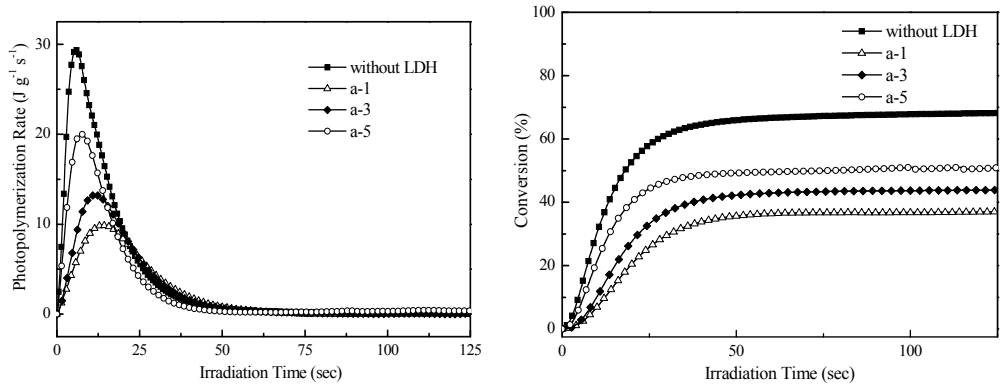

Fig. 4. Photopolymerization rates and unsaturation conversion of series A formulations.

However, for the series B samples, as shown in Fig. 5, the R_p^{max} and P^f are comparable with those for the pure resin without LDH addition. This might be interpreted that the additional 1173 plays a dominative role in initiating the photopolymerization. However, the R_p^{max} and P^f decrease slightly as the LDH increased because of the higher viscosity of series B samples than the pure resin.

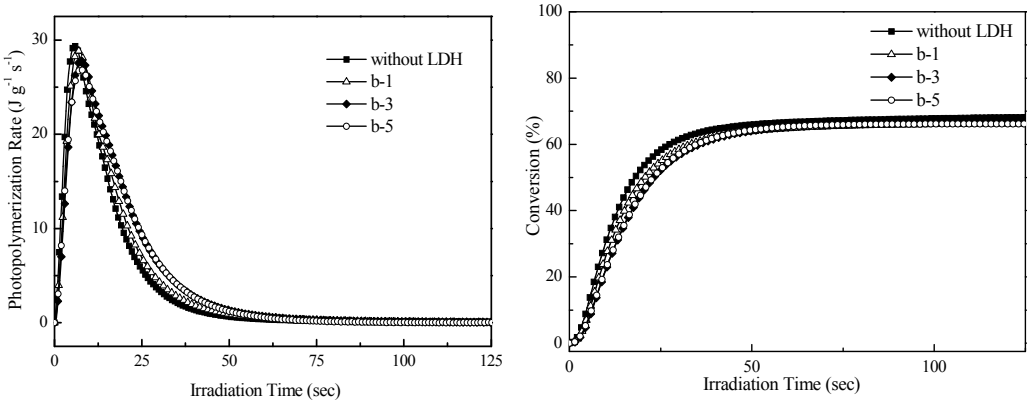

Fig. 5. Photopolymerization rates and unsaturation conversion of series B formulations.

3.3. Photopolymerization behavior of UV-curable urethane diacrylate/LDH blends

The photopolymerization rates at the peak maximum (R_p^{max}) and the final conversion of double bond (P^f) of the pure resin and urethane diacrylate/LDH blends are shown in Fig. 6. It can be seen that the R_p^{max} decreases slightly and the irradiation time to reach to the R_p^{max} is a little longer with increasing LDH content. The final unsaturation conversion also decreases in some sort with increasing LDH content. This can be explained by the fact that the urethane diacrylate/LDH blends have a lower concentration of double bond and higher viscosity compared with the pure resin. However, the tiny difference of R_p^{max} and P^f indicates the fine compatibility between the LDH-KH-24 and the pure resin.

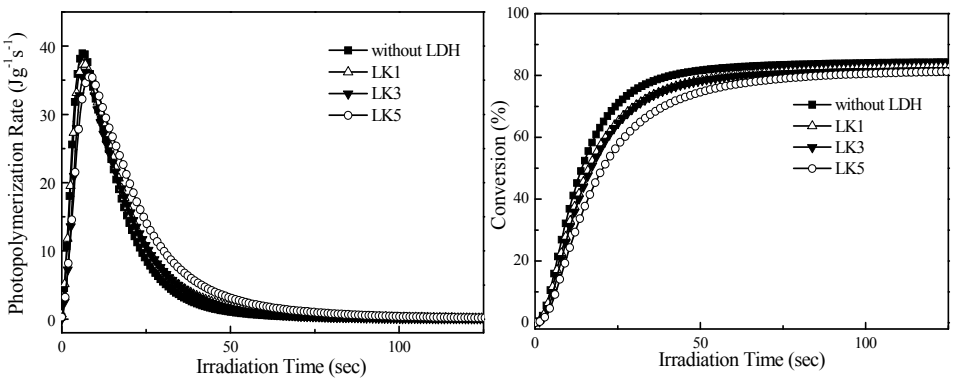

Fig. 6. Photopolymerization rates and unsaturation conversion of the LDH-KH formulations.

3.4. Morphology of the UV cured nanocomposites

To investigate the microstructures of UV cured polymer/LDH nanocomposite, the TEM micrographs of samples at 5 wt% LDH-1173 loading with and without additional 1173 are shown in Fig. 7. The dark lines are intersections of LDH platelets. The polymer/LDH nanocomposite shows the good dispersion of LDH in the polymer matrix (Fig. 7a. and Fig. 7c.). Moreover, for a-5, the LDH lost the ordered stacking-structure and are completely exfoliated when UV cured (Fig. 7b.). However, for b-5, the LDH was just intercalated by the polymeric chains, remaining the ordered structure (Fig. 7d.). This can be explained that for the sample a-5 produced by using only LDH-1173 in the interlayer, the content of photoinitiator was relative lower for initiating the photopolymerization of oligomers and monomers, resulting in the lower photopolymerization rate and double bond conversion (Fig. 5 and Fig. 6). On the other hand, however, the slow polymerization rate was propitious to the LDH intergallery further enlarged, and finally exfoliated. Whereas, for the sample b-5 produced by using not only LDH-1173 in the interlayer, but also the additional 3 wt% 1173, the higher photopolymerization rate and double bond conversion were obtained. However, the formed cross-link network from the fast curing retarded the interlayer spacing enlarging, and then finally forming the intercalated microstructure.

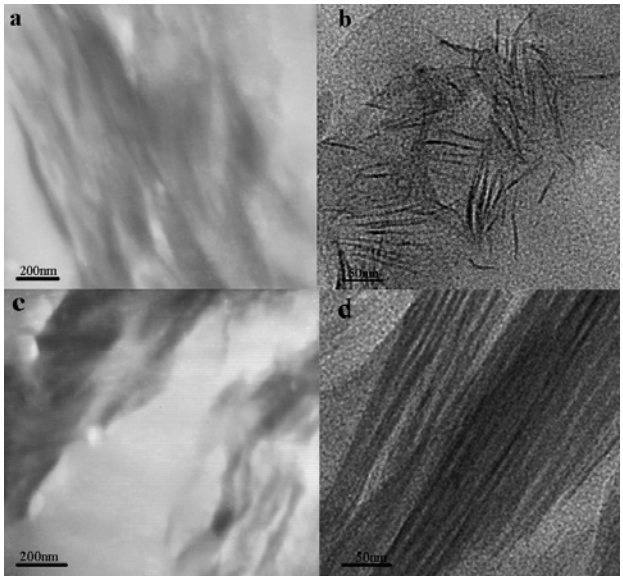

Fig. 7. TEM and HR-TEM micrographs of UV cured nanocomposites at 5 wt% LDH-1173 loading for a-5 (a, b) and b-5 (c, d).

To confirm the exact microstructure of the UV-cured polymer/LDH nanocomposite, the TEM micrograph of the samples at 5 wt% LDH-KH-24 loading is presented in Fig. 8. The TEM results demonstrate that LDH modified by SDS and KH570 has completely exfoliated during the curing process, because the previous modification of LDH not only enlarges the layer distance but also applies the reactive groups in the interlayer for further photopolymerization.

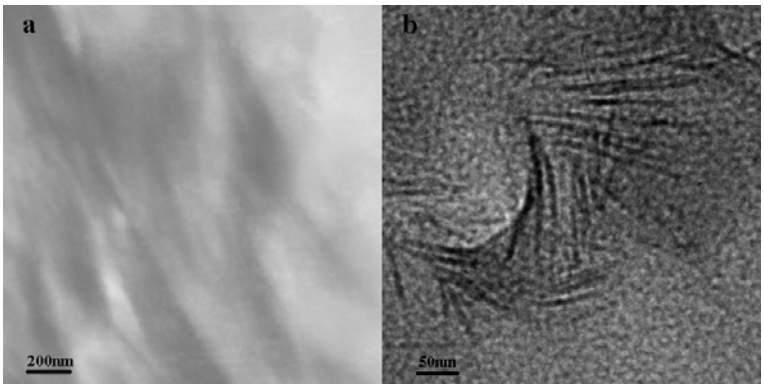

Fig. 8. TEM and HR-TEM micrographs of UV cured polymer/LDH nanocomposites at 5 wt% LDH loading.

3.5. Thermal properties of the UV cured nanocomposites

Fig. 9 shows the TGA curves of UV cured pure polymer and polymer/LDH nanocomposites with LDH-1173 and LDH-KH loading. As shown in the figure, the thermal decomposition trend of the nanocomposites is very similar to the pure polymer. As anticipated, the addition of LDH raised the onset temperature of thermal decomposition. Moreover, as the LDH loading increased, the char residue also increases, indicating that the LDH promoted the charring process. As a result, the thermal stability of polymer/LDH nanocomposites is improved by the addition of LDH-1173 and LDH-KH.

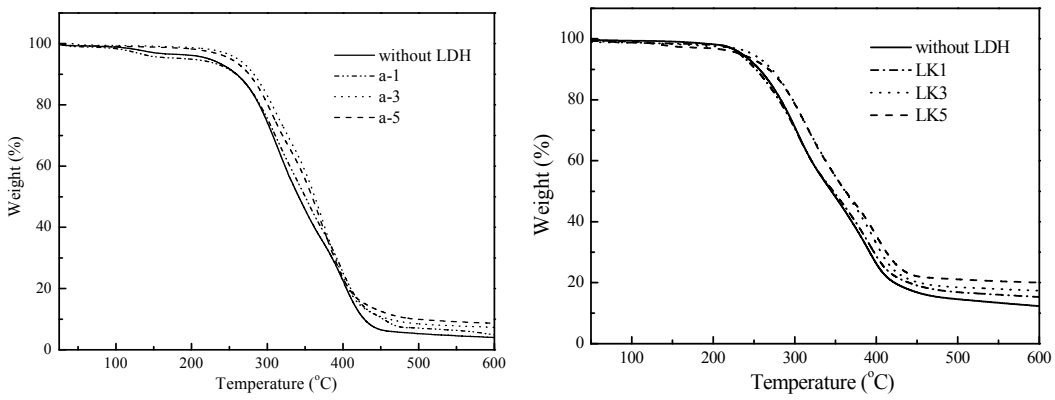

Fig. 9. TGA curves of UV cured polymer and nanocomposites with LDH-1173 and LDH-KH under N_2 flow.

The dynamic mechanical thermal analysis (DMTA) was used to investigate the mechanical properties of UV-cured polymer/LDH nanocomposites for further confirming the formed microstructure of nanocomposites. The T_g is determined as the peak temperature of the tanδ curve. From the DMTA data listed in Table 1, the addition of LDH-1173 causes a rise of T_g from 66.0 to 73.8 °C and a small increase of the storage modulus (E'). This can be explained by its exfoliation morphology with fine dispersion of LDH in the polymer matrix, which provides a large surface area

for LDH interacting with polymer matrix, leading to the restricted segmental motions near the organic-inorganic interfaces. It is also due to be the increase in the crosslink density (XLD) with increasing LDH-1173 content. The E' and glass transition temperature (T_g) of series A samples are a little higher than those of series B samples. This can be attributed to the exfoliation behavior of the former compared to the intercalated behavior of the latter.

Table 1. E', T_g and XLD of UV cured polymer and polymer/LDH nanocomposites with LDH-1173 addition from DMTA.

Sample	E'(pa)	T_g(°C)	XLD (mol cm^{-3})
Pure polymer	3.59×10^{7}	66.0	3.59×10^{-3}
a-1	4.21×10^{7}	67.0	4.21×10^{-3}
a-3	4.97×10^{7}	70.8	4.94×10^{-3}
a-5	5.01×10^{7}	73.8	4.97×10^{-3}
b-1	3.89×10^{7}	66.1	3.90×10^{-3}
b-3	4.31×10^{7}	67.8	4.23×10^{-3}
b-5	4.76×10^{7}	69.8	4.65×10^{-3}

The E' and $\mathbf{T_g}$ of the pure polymer and the nanocomposites LK1, LK3 and LK5 are listed in Table 2. The E' of the cured nanocomposites increases in some sort with the LDH addition increasing, while the XDL also increases with the LDH addition. These can be attributed to the good dispersion of LDH-KH in the polymer matrix during the UV-curing process and the increase of the effective degree of cross-linking. From the figure, the addition of LDH-KH-24 causes a tiny rise of T_g from 66.0 to 67.8 °C. This can be explained by the exfoliation morphology of LDH in the polymer matrix and the higher XDL of the nanocomposites, leading to the restricted segmental motions.

Table 2. DMTA results of UV cured polymer and nanocomposites.

Sample	E'(pa)	T_g (^{o}C)	XLD (mol/cm^{-3})
Pure polymer	3.97×10^{7}	66.0	3.94×10^{-3}
LK1	4.35×10^{7}	66.4	4.32×10^{-3}
LK3	4.36×10^{7}	66.7	4.34×10^{-3}
LK5	4.75×10^{7}	67.8	4.72×10^{-3}

3.6. Mechanical properties and hardness of UV-cured nanocomposites

The mechanical properties and hardness of UV cured polymer/LDH nanocomposites are listed in Table 3. The tensile strength of nanocomposites increases with the increase of LDH-1173 loading. Moreover, the tensile strength of series A nanocomposites is much higher than series B. This is in agreement with the results obtained by DMTA, where the E' value increases with the same trend. All the nanocomposites possess the acceptable percent elongation at break. The slight decrease in the elongation is reasonable, and can be explained that the polymer chains in the nanocomposite were restricted by the exfoliated LDH, resulting in the degree of freedom decreasing. The pendulum and pencil hardness of the nanocomposites films were measured, as listed in Table 3. Compared with the pure polymer film, the pendulum and pencil hardness both increase with increasing LDH loading in the nanocomposites, for both series A and B. As well known, the hardness of a nanocomposite is correlated not only with the inorganic component, but also with the crosslink network density. Therefore, the enhancement in hardness of the nanocomposites can be explained by the good

compatibility of LDH-1173 with the polymer matrix and the effective cross-linking reaction occurred in the UV curing polymer/LDH system. For the UV cured polymer/LDH nanocomposites with LDH-KH addition the same increase trend in mechanical properties and hardness was found with the nanocomposites containg LDH-1173.

Table 3. Mechanical properties and hardness of UV cured polymer and nanocomposites.

Sample	Tensile strength (Mpa)	Elongation at break (%)	Persoz Hardness (s)	Pencil hardness
Pure polymer	8.5	19	88	2H
a-1	12.2	17	95	2H
a-3	17.6	16	101	3H
a-5	21.4	16	114	4H
b-1	8.7	17	97	2H
b-3	8.9	17	103	3H
b-5	9.3	16	117	4H

4. Conclusion

The novel polymer/LDH nanocomposite were prepared through intercalating a photoinitiator 1173 or KH570 into the modified MgAl-LDH, forming the LDH-1173, or LDH-KH. The exfoliated UV cured polymer/LDH nanocomposites were acquired with LDH-1173 adding only, comparing with the intercalated polymer/LDH nanocomposites photoinitiated with both LDH-1173 and pure photoinitiator 1173. Moreover, the oragno-modified LDH, LDH-KH, was synthesized by intercalated a long alkyl surfactant and a silane coupling agent into LDH. The LDH-KH had a large basal spacing of 2.41 nm and showed the good compatibility with the acrylate resin. The exfoliated polymer/LDH nanocomposites exhibited better thermal stability, mechanical properties and higher hardness than the pure polymer. Moreover, the percent elongation at break also increased slightly due to the toughen effect of silane intercalated into the LDH interlayer.

Acknowledgements

This work was supported by the National Natural Science Foundation of China (Grant No. 50973100).

Refenrences

[1] W. Chen, B.J. Qu, Chem. Mater. 15 (2003) 3208-3213.
[2] Y.H. Yu, C.Y. Lin, J.M. Yeh, W.H. Lin, Polymer 44 (2003) 3553-3560.
[3] M. Malinconico, P. Laurienzo, Biomacromolecules 8 (2007) 773-779.
[4] L.Z. Qiu, W. Chen, B.J. Qu, Polymer 47 (2006) 922-930.
[5] C.S. Triantafillidis, P.C. Lebaron, T.J. Pinnavaia, Chem. Mater. 14 (2002) 4088-4096.
[6] G.A. Wang, C.C. Wang, C.Y. Chen, Polymer 46 (2005) 5065-5074.
[7] C.H. Tseng, H.B. Hsueh, C.Y. Chen, Compos. Sci. Technol. 67 (2007) 2350-2362.
[8] H.D. Peng, W. Tjiu, L. Shen, T.X. Liu, Compos. Sci. Technol. 69 (2009) 991-996.
[9] M. Adachi-Pagano, C. Forano, J. Besse, Chem. Commun. 1 (2000) 91-92.

[10] F. Leroux, M. Adachi-Pagano, M. Zatissar, S. Chauviere, C. Forano, J.P. Besse, J. Mater. Chem. 11 (2001) 105-112.
[11] T. Hibino, W. Jones, J. Mater. Chem. 11 (2001) 1321-1323.
[12] F.R. Costa, A. Leuteritz, U. Wagenknecht, M.A. der Landwenhr, D. Jehnichen, L. Haeccssler, G. Heinrich, Appl. Clay. Sci. 44 (2009) 7-14.
[13] C. Nyambo, E. Kandare, C.A. Wilkie, Polym. Degrad. Stabil. 94 (2009) 513-520.
[14] L.C. Du, B.J. Qu, Y.Z. Meng, Q. Zhu, Compos. Sci. Technol. 66 (2006) 913-918.
[15] A. Illaik, C. Vuillermoz, S. Commereusc, C. Taviot-Gueho, V. Verney, F. Leroux, J. Phys. Chem. Solids 69 (2008) 1362-1366.
[16] S.C. Lv, W. Zhou, H. Miao, W.F. Shi, Prog. Org. Coat. 65 (2009) 450-456.